Energetic and Structural Study of Diphenylpyridine Isomers

Marisa A. A. Rocha,[†] Lígia R. Gomes,[‡,§] John N. Low,[||] and Luís M. N. B. F. Santos*[,†]

Centro de Investigação em Química, Faculdade de Ciências, Universidade do Porto, R. do Campo Alegre 687, P-4169-007 Porto, Portugal, REQUIMTE—Departamento de Química, Faculdade de Ciências, Universidade do Porto, R. do Campo Alegre 687, P-4169-007 Porto, Portugal, CIAGEB, Faculdade de Ciências da Saúde da UFP, Universidade Fernando Pessoa, R. Carlos da Maia 296, P-4200-150 Porto, Portugal, and Department of Chemistry, University of Aberdeen, Meston Walk, Old Aberdeen AB24 3UE, Scotland

Received: April 24, 2009; Revised Manuscript Received: August 24, 2009

The energetic and structural study of three diphenylpyridine isomers is presented in detail. The three isomers, 2,6-, 2,5-, and 3,5-diphenylpyridines, were synthesized via Suzuki—Miyaura methodology based on palladium catalysis, and the crystal structures of the isomers were obtained by X-ray diffraction. The relative energetic stabilities in the condensed and gaseous phases as well as volatilities and structures of the three studied isomers were evaluated, regarding the position of the phenyl groups relative to the nitrogen atom of the pyridine ring. The temperature, standard molar enthalpies, and entropies of fusion were measured and derived by differential scanning calorimetry. The vapor pressures of the considered isomers were determined by a static apparatus based on a MKS capacitance diaphragm manometer. The standard molar enthalpies, entropies, and Gibbs energies of sublimation, at $T = 298.15$ K, were derived, and the phase diagram near the triple point coordinates were determined for all isomers. The standard ($p° = 0.1$ MPa) molar enthalpies of combustion of all crystalline isomers were determined, at $T = 298.15$ K, by static bomb combustion calorimetry. The standard molar enthalpies of formation, in the crystalline and gaseous phases, at $T = 298.15$ K, were derived. The experimental results for the energetics in the gaseous phase of the three compounds were compared and assessed with the values obtained by ab initio calculations at different levels of theory (DFT and MP2) showing that, at this level of theory, the computational methods underestimate the energetic stability, in the gaseous phase, for these molecules. In order to understand the aromaticity in the central ring of each isomer, calculations of NICS (B3LYP/6-311G++(d,p) level of theory) values on the pyridine ring were also performed.

Introduction

Substituted pyridines show a wide spectrum of biological activities which have been known for more than 70 years.[1] Nevertheless, with the genetic and proteomic revolution, new applications for these types of compounds has been found in the biological field. For instance, 2,5- and 3,5-disubstituted pyridine derivatives have been prepared and tested as a class of small molecules capable of controlling gene dynamics and expression, by regulation of the replication and transcription of DNA.[2]

Pharmacological activities, or the lack thereof, are usually attributed to geometric constraints, imposed by the shape or volume of the substituent on the pyridine ring. Although geometric features can explain satisfactorily the intensity of substrate-active site interactions, not many studies on electronic properties, focused on the relation between structure and activity in the pharmacological field, have been conducted so far. However, in past decades, a renewed interest in these compounds has arisen, due to their potential applications in the electronic industry. This has necessitated a deeper study of their electronic characteristics. Due to their π electronic structure, phenylpyridines and polyphenylpyridines are considered to be potential organic semiconductors; hence the research interest in this type of molecular system is primarily directed toward applications in areas such as organic light emitting devices (OLEDs), organic field effect transistors (OFETs), and organic photovoltaic cells (OPVCs). 2,5-Diphenylpyridine and its derivatives turn out to be optically active components in the liquid crystal phase, and some 2,6-diphenylpyridine-based compounds exhibit fluorescence in the blue-green region.[3]

Thus, because of the potential semiconductor capabilities of these materials, it is of fundamental importance to study their molecular structures, their thermodynamic properties, in both the condensed and gaseous phases, and their phase transition equilibria.

This article reports on a combined experimental energetic and structural study of some diphenylpyridine isomers, namely, 2,6-diphenylpyridine (2,6-DPhPy), 2,5-diphenylpyridine (2,5-DPhPy), and 3,5-diphenylpyridine (3,5-DPhPy), as illustrated in Figure 1.

The energetic differentiation in the condensed and gaseous phase evaluation, occurring with the change in the position of the phenyl groups relative to the heteroatom at the pyridine ring, was based on the interpretation of the experimental results for relative energetic stabilities, phase transition diagrams, and structural data. The energetics in the gaseous phase of all isomers was additionally analyzed by means of ab initio calculations, and a comparative and differential analysis between the experimental and theoretical results was performed.

* Corresponding author. Tel.: +351 220 402 836. Fax: +351 220 402 659. E-mail: lbsantos@fc.up.pt.

[†] Centro de Investigação em Química, Faculdade de Ciências, Universidade do Porto.

[‡] REQUIMTE—Departamento de Química, Faculdade de Ciências, Universidade do Porto.

[§] Universidade Fernando Pessoa.

[||] University of Aberdeen.

10.1021/jp903792d CCC: $40.75
Published on Web 09/17/2009

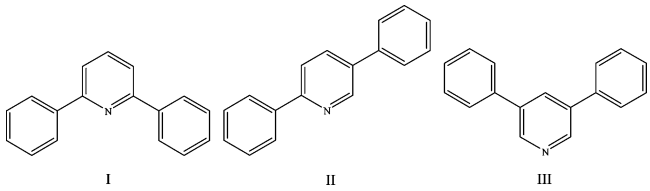

I II III

Figure 1. Structural formulas of I, 2,6-diphenylpyridine (2,6-DPhPy); II, 2,5-diphenylpyridine (2,5-DPhPy); and III, 3,5-diphenylpyridine (3,5-DPhPy).

The present work is part of a broader research project related to conducting polymers, which contributes to the understanding of the energetic effects of structural changes of attached phenyl groups relative to the nitrogen atom of the pyridine ring. Ribeiro da Silva et al. presented a thermochemical and theoretical study of the three phenylpyridine isomers, where the relative energetic stabilities in the gaseous phase, estimated by ab initio calculations, were in good agreement with experimental data.[4]

The three isomers, 2,6-DPhPy, 2,5-DPhPy, and 3,5-DPhPy, were synthesized via the Suzuki−Miyaura method based on palladium catalysis, and characterized by gas chromatography, elemental analysis, single crystal X-ray diffractometry, (^{1}H) nuclear magnetic resonance spectroscopy, and UV−vis spectroscopy. The fusion temperatures and the standard molar enthalpies of fusion were measured by differential scanning calorimetry (DSC). The standard molar enthalpies of sublimation and the enthalpy change due to the heating of the sample, in the condensed phase, from $T = 298.15$ K to T, were measured using the Calvet microcalorimetry drop-method. The thermodynamic parameters concerning sublimation were also obtained indirectly, based on vapor pressures determined at different temperature intervals [2,6-DPhPy(l), 360−400 K; 2,5-DPhPy(cr), 407−436 K; and 3,5-DPhPy(cr), 369−400 K], by a static apparatus based on an MKS capacitance diaphragm manometer. The standard ($p^\circ = 0.1$ MPa) molar enthalpies of formation in the crystalline phase of all isomers, at $T = 298.15$ K, were determined by static bomb combustion calorimetry. The standard molar enthalpies of formation in the gaseous phase were derived by the combination of the standard molar enthalpies of formation in the crystalline phase and the standard molar enthalpies of sublimation for each respective isomer. The ab initio evaluation of the energetics in the gaseous phase was based on density functional theory and on second-order Møller−Plesset perturbation theory. For the three studied compounds, the nucleus-independent chemical shift (NICS) scan profiles at the center of the pyridine ring were calculated from −2 to +2 Å, at the B3LYP/6-311++G(d,p) level of theory.

Experimental Section

Synthesis and Characterization of Compounds. The compounds 2,6-DPhPy [CAS Registry Number 3558-69-8], 2,5-DPhPy [CAS Registry Number 15827-72-2], and 3,5-DPhPy [CAS Registry Number 92-07-9] were synthesized using the Suzuki−Miyaura cross-coupling reaction based on palladium catalysis.[5] The reactions were optimized for a ratio of water and dimethylformamide of 3.5:3 (2,6-DPhPy and 3,5-DPhPy) and for a ratio of water and toluene of 4:2 (2,5-DPhPy). As schematically represented in Figure 2, a mixture of K_2CO_3 (6 mmol), $Pd(OAc)_2$ (0.01 mmol), and respectively dibromopyridine (1 mmol), phenylboronic acid (4 mmol), water, and organic solvent was stirred for approximately 8 h at 373 K. The resulting crude solid was purified by recrystallization from ethanol. Dibromopyridines, phenylboronic acid, and $Pd(OAc)_2$ were acquired from Aldrich Chemical Co.

The three solid isomers were purified by successive recrystallization in methanol and several vaporization cycles, with 2,6-DPhPy at $T = 413$ K, or successive sublimation, under reduced pressure (<10 Pa), 2,5-DPhPy at $T = 403$ K, and 3,5-DPhPy at $T = 405$ K.

The final purity of the samples was verified by gas chromatographic analysis, using an HP 4890 apparatus equipped with an HP-5 column, cross-linked, 5% diphenyl and 95% dimethylpolysiloxane. The mass fractions of the pure compounds were as follows: 2,6-DPhPy 0.9997; 2,5-DPhPy 0.9996; 3,5-DPhPy 0.9998.

For the mass fraction, w, determined by elemental analysis of C, H, and N, the following was found: for 2,6-diphenylpyridine, $C_{17}H_{13}N$, $w(C) = 88.6$, $w(H) = 5.4$, $w(N) = 6.0$; for 2,5-diphenylpyridine, $C_{17}H_{13}N$, $w(C) = 88.3$, $w(H) = 5.5$, $w(N) = 6.2$; for 3,5-diphenylpyridine, $C_{17}H_{13}N$, $w(C) = 88.4$, $w(H) = 5.5$, $w(N) = 6.1$, calculated $w(C) = 88.28$, $w(H) = 5.67$, $w(N) = 6.06$.

The ^{1}H NMR ($CDCl_3$, TMS), spectra were taken in a Bruker AMX-300 instrument (300 MHz). ^{1}H NMR ($CDCl_3$, 300 MHz): for 2,6-diphenylpyridine, 8.15−8.30 (d, 4H, phenyl), 7.85−7.72 (t, 1H, pyr), 7.69−7.55 (d, 2H, pyr), 7.54−7.45 (m, 6H, phenyl); for 2,5-diphenylpyridine, 9.02−8.91 (s, 1H, pyr), 8.23−8.00 (d, 2H, phenyl), 8.05−7.89 (d, 1H, pyr), 7.85−7.78 (d, 1H, pyr), 7.68−7.60 (d, 2H, phenyl), 7.56−7.45 (m, 2H, phenyl); for 3,5-diphenylpyridine, 9.02−8.85 (s, 2H, pyr), 8.10−8.05 (s, 1H, pyr), 7.72−7.59 (d, 4H, phenyl), 7.59−7.45 (m, 6H, phenyl).

The relative atomic masses used were those recommended by the IUPAC Commission in 2005.[6]

X-ray Diffractometry. The data acquisition was made using a Bruker SMART APEX diffractometer equipped with data collection (APEX2), cell refinement (APEX2 and SAINT), and data reduction (SAINT) programs.[7] Numerical absorption correction was performed with Multiscan SADABS 2.10.[8] SHELX-97[9] was used to carry out the structure solution and refinement.

The structures were solved by direct methods and subsequent Fourier difference techniques. All non-hydrogen atoms were refined anisotropically by full-matrix least-squares on F^2 as implemented in SHELX-97. 3,5-DPhPy crystallized in the monoclinic system, space group $C2/c$ or Cc from the systematic absences. $C2/c$ was assumed and confirmed by the analysis. H atoms were treated as riding atoms with C−H(aromatic), 0.95 Å. 2,6-Diphenylpyridine crystallized in the monoclinic system and space group $P21/c$ was assumed from the systematic absences. It was refined using a model where the central ring is disordered over two sites at 50% each and the N atom is distributed around each disordered ring (the occupancies of the C and N at each site are 0.375 and 0.125, respectively), as imposed by the symmetry. This disordered model was found to give the lowest R-factor by a process of varying the percentage of each conformer present; the N atom was assumed to be uniformly disordered around the ring. The positions of the C and N atoms at each site were fixed to have the same coordinates and were given fixed anisotropic thermal parameters for each disordered ring based on one C atom in each ring. H atoms of the central ring were calculated on the basis of the disorder. H atoms were treated as riding atoms with C−H(aromatic), 0.95 Å. Crystal data, data collection, and refinement details for 2,5-DPhPy and 3,5-DPhPy are presented in Table 1.

Molecular and packing diagrams were generated by ORTEP[10] and PLATON.[11]

UV−Vis Spectroscopy. UV−vis spectra were measured using a diode array spectrophotometer, an Agilent 8453 UV−visible spectroscopy system with temperature control. For

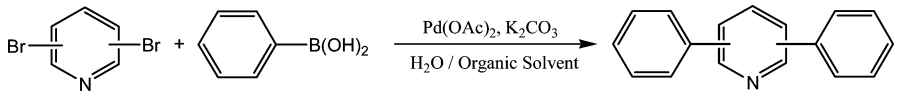

Figure 2. Scheme of the reaction procedure used in the syntheses based on the Suzuki−Miyaura cross-coupling reaction.

TABLE 1: Crystal Data and Structure Refinement for 3,5-Diphenylpyridine and 2,5-Diphenylpyridine

	2,5-DPhPy	3,5-DPhPy
empirical formula	$C_{17}H_{13}N$	$C_{17}H_{13}N$
formula weight	$M_r = 231.28$ mol·dm^{-3}	$M_r = 231.28$ mol·dm^{-3}
temp/K	123 (2) K	123 (2) K
λ/Å	0.710 73 Å	0.710 73 Å
crystal system	monoclinic, *P*21/*c*	monoclinic, *C*2/*c*
cell constants	$a = 13.5073$ (6) Å, $b = 5.5571$ (2) Å, $c = 7.8721$ (4) Å, $\beta = 92.170$ (3)°	$a = 26.8480$ (11) Å, $b = 6.4901$ (3) Å, $c = 7.2411$ (3) Å, $\beta = 102.297$ (2)°
volume	$V = 590.47$ (5) Å^3	$V = 1232.79$ (9) Å^3
molecules per unit cell, *Z*	2	4
D_x	1.301 mg m^{-3}	1.246 mg m^{-3}
F(000)	244	488
crystal size (shape, color)	0.20 × 0.20 × 0.01 mm (plate, colorless)	0.20 × 0.20 × 0.010 mm (plate, colorless)
θ range for data collection	3.02−27.5°	1.6−29.1°
cell parameters	from 6687 reflections	from 1405 reflections
absorption coefficient	$\mu = 0.076$ mm^{-1}	$\mu = 0.075$ mm^{-1}
radiation source	fine-focus sealed tube	fine-focus sealed tube
monochromator	graphite	graphite
θ range	$\theta_{min} = 3.1°$; $\theta_{max} = 30.5°$; ω scans	$\theta_{min} = 3.1°$; $\theta_{max} = 30.5°$; ω scans
limiting indices	$h = -17 \rightarrow 16$, $k = -7 \rightarrow 7$, $l = -10 \rightarrow 10$	$h = -38 \rightarrow 38$, $k = -9 \rightarrow 9$, $l = -10 \rightarrow 10$
reflections collected/unique	6687/1355; 1088 with $I > 2\sigma(I)$; $R_{int} = 0.047$	6243/1850; 1546 with $I > 2\sigma(I)$; $R_{int} = 0.042$
max and min transmission	$T_{min} = 0.985$, $T_{max} = 0.993$	$T_{min} = 0.986$, $T_{max} = 0.999$
data/restraints/parameters	1355/0/88	1850/0/83
goodness of fit on F^2	1.081	1.040
final *R* indices	$R[F^2 > 2\sigma(F^2)] = 0.0468$; $wR(F^2) = 0.1356$	$R[F^2 > 2\sigma(F^2)] = 0.0481$; $wR[(F^2 > 2\sigma(F^2)] = 0.1248$
final *R* indices (all data)	$R = 0.0573$; $wR(F^2) = 0.1475$	$R = 0.0584$; $wR(F^2) = 0.1366$
$\Delta\rho_{max}$, $\Delta\rho_{min}$	0.37 e Å^{-3} and −0.17 e Å^{-3}	0.43 e Å^{-3} and −0.24 e Å^{-3}
refinement method	full matrix least-squares on F^2	full matrix least-squares on F^2
CCDC No.	722316	690365

the three compounds, the measurements were performed using ethanol (Pronalab p.a.) as a solvent, and quartz cells as cuvettes. The UV−vis spectra were measured over the range from 200 to 700 nm, at a temperature of 298 K.

Differential Scanning Calorimetry. The temperatures and the standard molar enthalpies of fusion for 2,6-DPhPy, 2,5-DPhPy, and 3,5-DPhPy were measured in a power compensation differential scanning calorimeter, SETARAM Model DSC 141, using a heating rate of 3.33×10^{-2} K·s^{-1}, and aluminum crucibles.

The temperature and heat flux scales were calibrated by measuring the temperature and the heat of fusion of naphthalene [CAS Registry Number 91-20-3], benzoic acid [CAS Registry Number 65-85-0; NIST Standard Reference Material 39j], *p*-anisic acid [CAS Registry Number 100-09-4], indium [CAS Number 7440-74-6], and tin [CAS Registry Number 7440-31-5].

From the experimental values of temperatures and the standard molar enthalpies of fusion, the standard molar entropies of fusion of each isomer were derived.

Calvet Microcalorimetry. The standard molar enthalpies of sublimation for the three compounds were measured in a high temperature Calvet microcalorimeter, Model SETARAM HT 1000D, using a technique similar to the drop method described by Skinner et al.[12] The measurement procedure and the description of the apparatus have been described in detail by Santos et al.[13] The experimental description of the typical experiment of Calvet microcalorimetry is available as Supporting Information.

The standard molar enthalpies of sublimation at $T = 298.15$ K were calculated from the experimental values of $\Delta_{cr,298.15\,K}^{g,T}H_m°$, at the temperature T of the hot zone, using the following equation:

$$\Delta_{cr}^{g}H_m°(T = 298.15\ \text{K}) = \Delta_{cr,298.15\,K}^{g,T}H_m° - \{H_m°(g, T) - H_m°(g, 298.15\ \text{K})\} \quad (1)$$

where the value of $\{H_m°(g, T) - H_m°(g, 298.15\ \text{K})\}$ represents the molar enthalpic correction for the respective heat capacity of the gaseous phase, which was estimated by statistical thermodynamics using the fundamental vibrational frequencies derived by computational thermochemistry at the B3LYP/6-311++G(d,p) level of theory. For the correction of anharmonicity, a scaling factor of 0.9688 was considered.[14]

The microcalorimeter was calibrated with anthracene at the respective temperatures of the experiments of 2,6-DPhPy, 2,5-DPhPy, and 3,5-DPhPy, using the standard molar enthalpy of sublimation of anthracene, $\Delta_{cr}^{g}H_m°(T = 298.15\ \text{K}) = (100.2 \pm 0.4)$ kJ·mol^{-1}.[15] The calibration constant of the calorimeter was found to be $k(T = 432\ \text{K}) = 0.9924 \pm 0.0046$, obtained from the average of six independent experiments, with the uncertainty being the standard deviation of the mean.

The enthalpy change due to the heating of the sample in the condensed phase from $T = 298.15$ K to the temperature of the microcalorimeter, T $\{H_m°(cd, T) - H_m°(cd, 298.15\ \text{K})\}$, was determined for each compound using a methodology similar to that described by Bernardes et al.[16] The values of $\{H_m°(cd, T) - H_m°(cd, 298.15\ \text{K})\}$ for 2,6-DPhPy, 2,5-DPhPy, and 3,5-DPhPy were measured using the Calvet microcalorimeter, Model SETARAM HT 1000D.

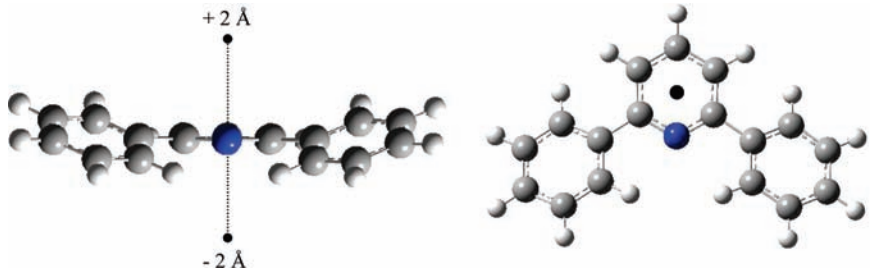

Figure 3. NICS probes placed above and below (from −2 to +2 Å, in increments of 0.2 Å) the geometric center of the pyridine ring of 2,6-diphenylpyridine.

Static Apparatus Based on a MKS Capacitance Diaphragm Manometer. The vapor pressures of 2,6-DPhPy, 2,5-DPhPy, and 3,5-DPhPy were measured at several temperatures, using the static apparatus based on an MKS capacitance diaphragm manometer recently described in detail.[17]

The vapor pressures were measured by a capacitance diaphragm absolute gauge MKS Baratron 631A01TBEH, capable of measuring in the pressure range of 0.4−133 Pa and in the temperature range of 253−423 K, and by a capacitance diaphragm absolute gauge MKS Baratron 631A11TBFP capable of measuring in the pressure range of 0.4−1333 Pa and in the temperature range of 253−473 K. To avoid condensation of the sample, the temperature of the vacuum line was maintained 10−20 K above the sample temperature. The vapor pressures of the mentioned compounds were measured at different temperature intervals: 2,6-DPhPy(l), 360−400 K; 2,5-DPhPy(cr), 407−436 K; and 3,5-DPhPy(cr), 369−400 K.

Combustion Calorimetry. The standard massic energies of combustion of the crystalline isomers of diphenylpyridine, 2,6-DPhPy, 2,5-DPhPy, and 3,5-DPhPy, were determined using an isoperibol static bomb calorimeter, with a twin valve bomb of internal volume of 0.290 dm^3, that had been formerly used at the National Physical Laboratory, Teddington, U.K.,[18] and in Manchester, U.K.[19] This calorimeter was transferred from Manchester to Porto, Portugal, and was used as previously described;[18,19] a few changes in the technique were applied.[20]

The calorimeter temperature was measured with a resolution of $\pm 2 \times 10^{-5}$ K in intervals of 10 s, with a calibrated ultrastable thermistor (Thermometrics Model S10) using a 7 1/2 digit nanoohmmeter (HP Model 34420A) interfaced to a computer programmed to compute the adiabatic temperature change based on the software LABTERMO V3.0.[21] The temperature readings were collected every 10 s, and the ignition temperature, for all experiments, was chosen in a way that the final temperature would be close to $T = 298.15$ K.

The calorimetric system was calibrated using benzoic acid (NIST Standard Reference Material 39j), having a massic energy of combustion under bomb conditions of (-26434 ± 3) J·g^{-1}.[22] From eight calibration experiments, the energy equivalent of the calorimeter, ε_{cal}, was found to be (15546.3 ± 1.3) J·K^{-1}, for an average of water of 2900.0 g added to the calorimeter, where the associated uncertainty refers to the standard deviation of the mean.

The crystalline samples of all isomers were burnt in oxygen at a pressure of 3.04 MPa, in the form of pellets, with a volume of 1.00 cm^3 of water added to the bomb. To promote complete combustion, benzoic acid (NIST Standard Reference Material 39j) and *n*-hexadecane (Aldrich Chemical Co., Gold Label) were used as auxiliary substances.

The electrical energy for ignition was derived from the change in potential difference across a 1400 μF condenser during discharge through a platinum ignition wire. The massic energy of combustion, for the cotton thread fuse with the empirical formula $CH_{1.686}O_{0.843}$, was assigned to $-16\,240$ J·g^{-1}.[23] The amount of nitric acid was determined by titration against NaOH. Corrections for nitric acid formation were based on −59.7 kJ·mol^{-1} for the molar energy of formation of 0.1 mol·dm^{-3} HNO_3(aq) from O_2, N_2, and H_2O(l).[24] For the studied compounds, an estimated pressure coefficient of massic energy, $(\partial u/\partial p)_T = -0.2$ J·g^{-1}·MPa^{-1}, at $T = 298.15$ K, a typical value for most organic compounds, was assumed.[25]

Standard-state corrections were calculated for the initial states by the procedures given by Hubbard et al.[26] and by Good and Scott.[27]

Computational Section

The computational calculations were executed using two different computational methods, i.e., density functional theory (DFT) with the hybrid exchange correlation functional (B3LYP)[28] and second-order Møller−Plesset perturbation theory (MP2).[29] The geometry optimizations and the fundamental vibrational frequency calculations were performed using the B3LYP method at the 6-311++G(d,p) level of theory. The geometry optimizations and the electronic energy were also calculated using the MP2 theory at the cc-pVDZ basis sets. The spin-component-scaled MP2 (SCS-MP2) electronic energies were also derived from the MP2/cc-pVDZ calculation according to the method proposed by Grimme.[29] The zero-point vibrational energies (ZPEs) and the fundamental vibrational frequencies were scaled using the scaling factors of 0.9887 and 0.9688, respectively.[14]

The assessment of aromaticity of the pyridine ring of the three diphenylpyridine isomers was performed using the NICS method. This method has been widely applied to evaluate the aromaticity of aromatic organic compounds.[30−32] The NICS probes (Bq) were placed at the geometric center of the pyridine ring, perpendicular to the average of the pyridine plane, from −2 to +2 Å, in increments of 0.2 Å. The NICS values were calculated for all ghost atoms using the standard GIAO procedure at the B3LYP/6-311++G(d,p) level of theory. The basis set used in the NICS calculations was found to be the minimum-quality basis set needed to satisfactorily derive NICS values.[33] Figure 3 presents the NICS probes placed above and below the geometric center of the pyridine ring of 2,6-diphenylpyridine.

All theoretical calculations were performed using the Gaussian 03 software package.[34]

Results and Discussion

X-ray Diffractometry. ***Crystal Structure of 2,5-Diphenylpyridine.*** Single crystals of 2,5-DPhPy were obtained by slow evaporation of a methanol solution. Bond distances, angles, and dihedral angles between the two distal rings obtained by X-ray

TABLE 2: Selected Geometric Parameters for 2,5-Diphenylpyridine

Bond Distances/Å	
C21−C22	1.3980 (15)
C21−C26	1.3985 (14)
C21−C2	1.4853 (15)
C22−C23	1.3878 (16)
C23−C24	1.3850 (16)
C24−C25	1.3834 (15)
C25−C26	1.3872 (15)
C2−N3A	1.336 (4)
C2−N3B	1.347 (5)
C2−N1A	1.383 (5)
C2−N1B	1.395 (5)
Bond Angles/deg	
C22−C21−C26	118.08 (10)
C22−C21−C2	121.21 (9)
C26−C21−C2	120.72 (9)
C23−C22−C21	120.77 (10)
C24−C23−C22	120.37 (10)
C25−C24−C23	119.59 (10)
C24−C25−C26	120.27 (10)
C25−C26−C21	120.92 (10)
C3A−C2−C3B	117.1 (2)
C3A−C2−C1A	113.2 (3)
C3B−C2−C1B	113.1 (3)
C1A−C2−C1B	118.9 (2)
C3A−C2−C21	121.2(2)
C3B−C2−C21	121.6 (2)
C1A−C2−C21	120.4 (2)
C1B−C2−C21	120.7 (2)
Dihedral Angles[a]/deg	
C26A−C21A−C21−C22	0.71 (11)
C26A−C21A−C21−C26	−180.00 (10)
C22A−C21A−C21−C22	179.98 (13)
C22A−C21A−C21−C26	−0.71 (11)

[a] Pseudo-dihedral angles between the two distal rings.

diffraction are presented in Table 2, and the ORTEP representation with the atom label scheme is depicted in Figure 4. The phenyl rings are planar, with the mean deviation of the six fitted carbons atoms to the best plane being 0.0020 Å. The central ring is disordered with the nitrogen atom having a quarter of the total site occupation for the −ortho and −meta positions of the heteroaromatic ring. The molecule presents two twisted conformations (identified with different labels in the central ring) that can be distinguished by the dihedral angle made between the coplanar aromatic phenyl rings with the pyridinic central ring. One of the possible conformations is more distorted than the other, with a dihedral angle of 20.36 (0.016)° compared with that of 6.03 (0.29)° for the more planar conformation. The two sites are separated by a rotation of 26.35 (0.25)°. The obtained structure is isomorphous with that of *p*-terphenyl (1,4-diphenylbenzene) obtained at 200 K. *p*-Terphenyl, as other polyphenyls, undergoes structural phase transitions that have been studied by X-ray and neutron diffraction as well as by NMR and EPR spectroscopies. At 200 K, the central phenyl ring seems to jump between two sites separated by a very similar rotation angle of 26.6° which is temperature independent, for values above the critical temperature.[35,36] The supramolecular structure of 2,5-DPhPy is stabilized by a very weak C−H···π interaction giving a herringbone pattern, as depicted in Figure 5, typical for aromatic hydrocarbon compounds.[37] The central ring of the 2,5-DPhPy isomer is so disordered that it is difficult to make any assumptions about the torsional angles of the phenyl rings. The pseudo-dihedral angles between the two distal rings, presented in Table 2, were used to evaluate the relative alignment of the distal rings. It was found that, despite the significant central ring disordering, the distal rings are in perfect parallel alignment.

Crystal Structure of 3,5-Diphenylpyridine. The molecular structure with the atom labeling scheme and the crystal packing

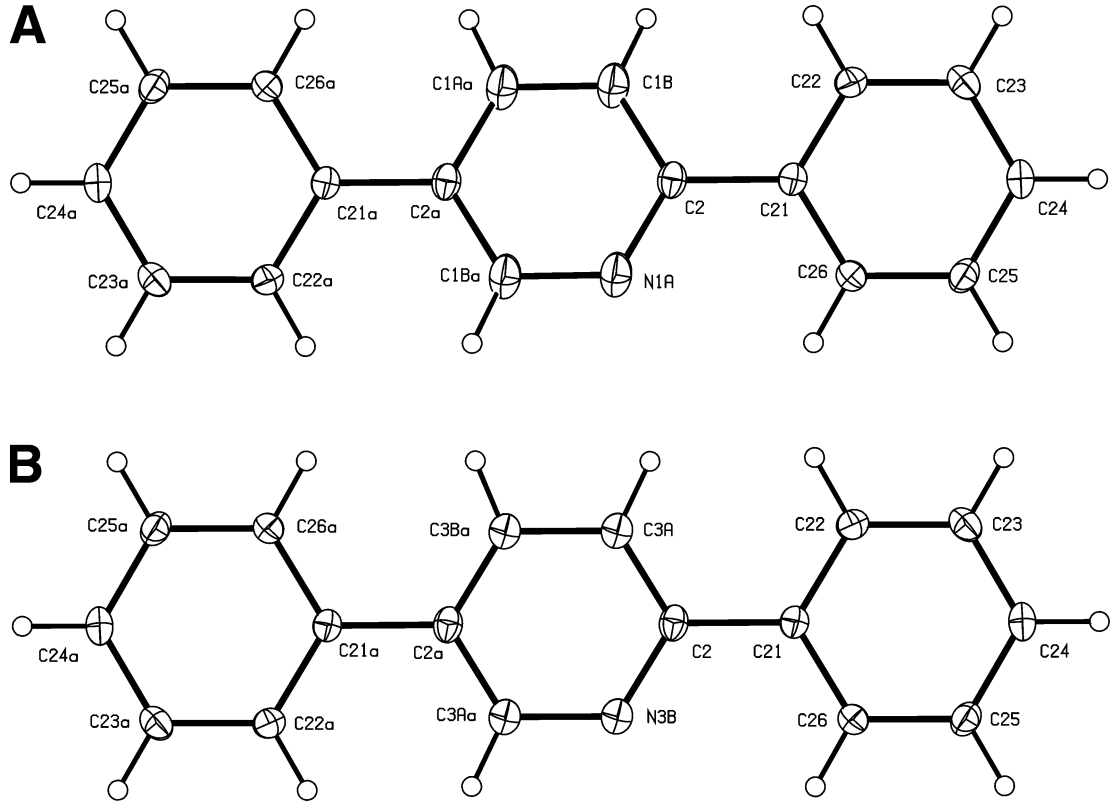

Figure 4. View of 2,5-diphenylpyridine, molecules A (with labels C1*x* in the central ring) and B (with labels C3*x* in the central ring), with displacement ellipsoids drawn at the 30% probability level (arbitrary spheres for the H atoms).

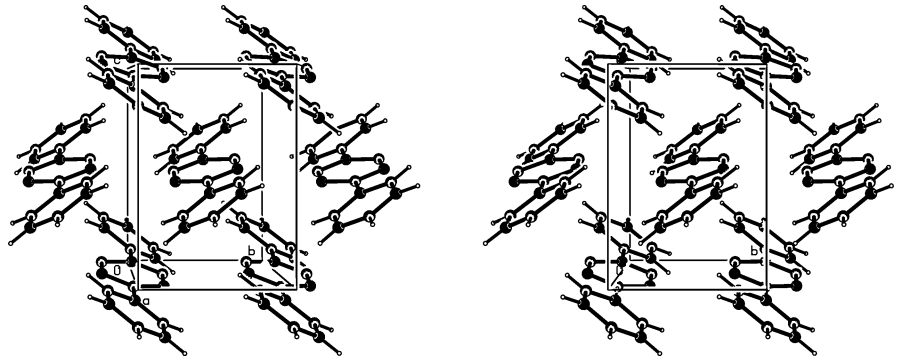

Figure 5. Molecular packing diagram for 2,5-diphenylpyridine (molecule A, top, and molecule B, bottom), showing the herringbone patterns obtained by C−H···π interaction.

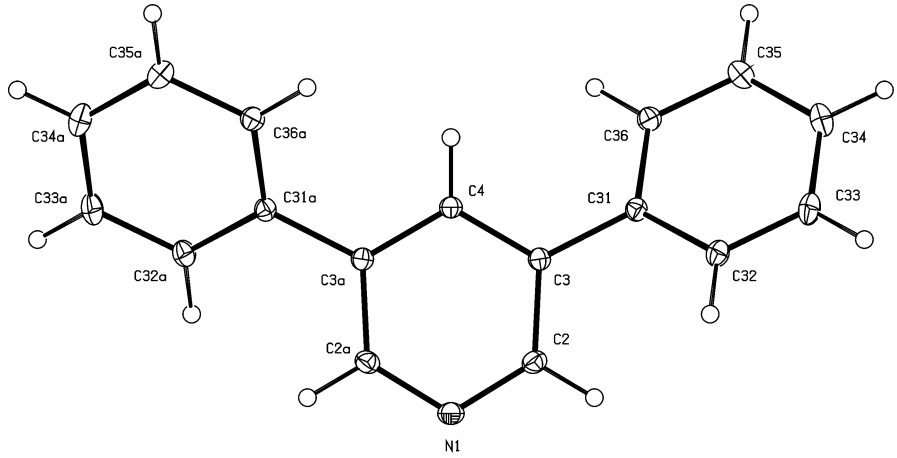

Figure 6. View of 3,5-diphenylpyridine with displacement ellipsoids drawn at the 30% probability level (arbitrary spheres for the H atoms).

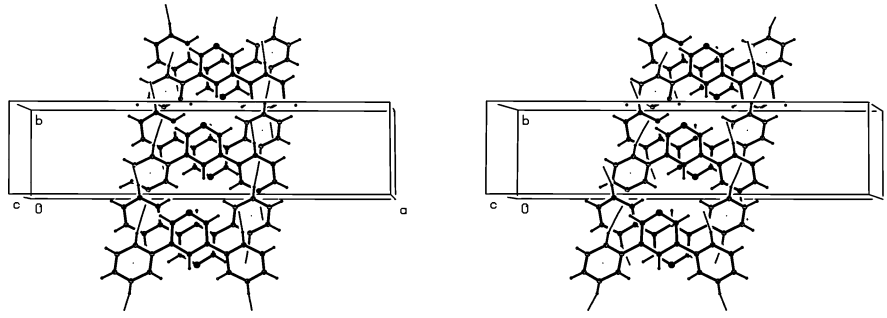

Figure 7. Stereoscopic view of symmetry-related chains of molecules of 3,5-diphenylpyridine linked by π···π interaction.

diagrams for 3,5-DPhPy are presented in Figures 6 and 7. Selected bond distances and angles are shown in Table 3. The bond distances and angles are in agreement with those previously described for similar compounds.[38,39]

The molecule lies on a 2-fold axis at (1/2, *y*, 1/4), with the axis passing through atoms N1 and C4. The discrete molecules are linked by π···π interactions between top adjacent folded pyridine rings with $d = 3.6791$ Å and by two weak C−H···π interactions, where the C32 and C35 carbon atoms of the molecule at (*x*, *y*, *z*) act as hydrogen donors via H32 and H35 to the center of gravity of the phenyl ring (Cg2) of the molecule placed at (x, $-y$, $1/2 + z$) and (x, $-y$, $-1/2 + z$), respectively, linking the molecules head to tail, forming sheets of molecules parallel to the [001] axis. The C32−H32 →Cg(2) and C35−H35 →Cg(2) distances are 2.78 and 2.73 Å, respectively. There are no interactions between adjacent sheets. There are no other types of interaction in the structure.

Crystal Structure of 2,6-Diphenylpyridine. In 2,6-DPhPy,[40] the molecules are linked only by a weak C−H···π interaction, leading to [011] chains.

UV−Vis Spectroscopy. The UV−vis spectra of 2,6-DPhPy, 2,5-DPhPy, and 3,5-DPhPy in ethanol solution are presented in Figure 8. 2,6-DPhPy shows three absorption bands with maximum absorptivity at 208, 235, and 299 nm. The absorptions at 235 and 299 nm correspond to the $\pi-\pi^*$ transition bands of the conjugated compound. The UV−vis absorption spectrum of 3,5-DPhPy is similar to the UV−vis absorption spectrum of 2,6-DPhPy, but only shows two absorption bands at 208 and 235 nm. The last absorption band corresponds to the $\pi-\pi^*$ transition of the conjugated compound. 2,5-DPhPy shows two absorption bands at 208 nm and a continuous absorption band at 262 nm, which corresponds to the $\pi-\pi^*$ transition of the conjugated compound. Comparing both UV−vis absorption spectra of 2,5-DPhPy and 2,6-DPhPy, it can be verified that 2,5-DPhPy undergoes a right shift of λ_{max}, which is indicative of an increase of the aromatic conjugation.

Phase Transition. The experimental fusion temperatures, standard molar enthalpies, and entropies of fusion, measured in a power compensation differential scanning calorimeter,

TABLE 3: Selected Geometric Parameters for 3,5-Diphenylpyridine[a]

Bond Distances/Å	
N1—C2	1.3369 (12)
N1—C2^{i}	1.3369 (12)
C2—C3	1.4013 (14)
C3—C4	1.3965 (12)
C3—C31	1.4835 (13)
C4—C3^{i}	1.3965 (12)
C31—C36	1.4014 (14)
C31—C32	1.4028 (14)
C32—C33	1.3914 (14)
C33—C34	1.3897 (17)
C34—C35	1.3916 (16)
C35—C36	1.3913 (14)
Bond Angles/deg	
C2—N1—C2^{i}	116.95 (13)
N1—C2—C3	124.26 (10)
C4—C3—C2	117.43 (10)
C4—C3—C31	122.79 (10)
C2—C3—C31	119.77 (9)
C3^{i}—C4—C3	119.60 (13)
C36—C31—C32	118.55 (9)
C36—C31—C3	121.05 (9)
C32—C31—C3	120.39 (9)
C33—C32—C31	120.45 (10)
C34—C33—C32	120.38 (10)
C33—C34—C35	119.76 (10)
C36—C35—C34	120.04 (11)
C35—C36—C31	120.79 (10)

[a] Symmetry codes: (i) $-x + 1, y, -z + 1/2$.

SETARAM Model DSC 141, for 2,6-DPhPy, 2,5-DPhPy, and 3,5-DPhPy are presented in table 4.

Considering experimental results obtained in a crystal−liquid equilibrium study of the three isomers, 2,6-DPhPy has a significantly lower enthalpy of fusion and a remarkably low fusion temperature compared with the other two isomers. These results are in agreement with the existing crystal packing constraints due to the weak intramolecular C−H···N interactions present in this isomer.

TABLE 4: Fusion Temperatures, T_{onset}, Standard Molar Enthalpies of Fusion, $\Delta^{l}_{cr}H_m^\circ$, and Standard Molar Entropies of Fusion, $\Delta^{l}_{cr}S_m^\circ$, of 2,6-DPhPy, 2,5-DPhPy, and 3,5-DPhPy

compound	T_{onset}/K	$\Delta^{l}_{cr}H_m^\circ(T_{onset})$/ kJ·mol^{-1}	$\Delta^{l}_{cr}S_m^\circ(T_{onset})$/ J·K^{-1}·mol^{-1}
2,6-DPhPy	354.41 ± 0.35	19.67 ± 0.87	55.5 ± 2.4
2,5-DPhPy	445.25 ± 0.92	30.26 ± 0.83	68.0 ± 1.9
3,5-DPhPy	409.18 ± 0.40	33.52 ± 1.20	81.9 ± 2.9

It can be observed that the fusion temperature of the 2,5-DPhPy isomer is significantly higher than that of the 3,5-DPhPy isomer; nevertheless, the standard molar enthalpy of fusion of 3,5-DPhPy is higher than the standard molar enthalpy of fusion of the 2,5-DPhPy isomer. The significantly higher temperature of fusion observed for the 2,5-DPhPy isomer is governed by the lower standard molar entropy of fusion for this isomer when compared with that of 3,5-DPhPy. The observed entropic differentiation is in good agreement with the additional entropic contribution associated with the central ring disorder observed in our X-ray crystal structure of 2,5-DPhPy.

The standard molar enthalpies of sublimation for the three isomers were obtained using a direct method (Calvet microcalorimetry) and an indirect method (static apparatus).

Table 5 lists the results of the measurements of the standard molar enthalpies of sublimation of the diphenylpyridine isomers, obtained by a high temperature Calvet microcalorimeter, as well as the respective uncertainties.

The enthalpy change due to the heating of the sample in condensed phase from $T = 298.15$ K to the programmed temperature, T, in the Calvet microcalorimeter, $\{H_m^\circ(\text{cd}, T) - H_m^\circ(\text{cd}, 298.15\ \text{K})\}$, is presented in Table 6.

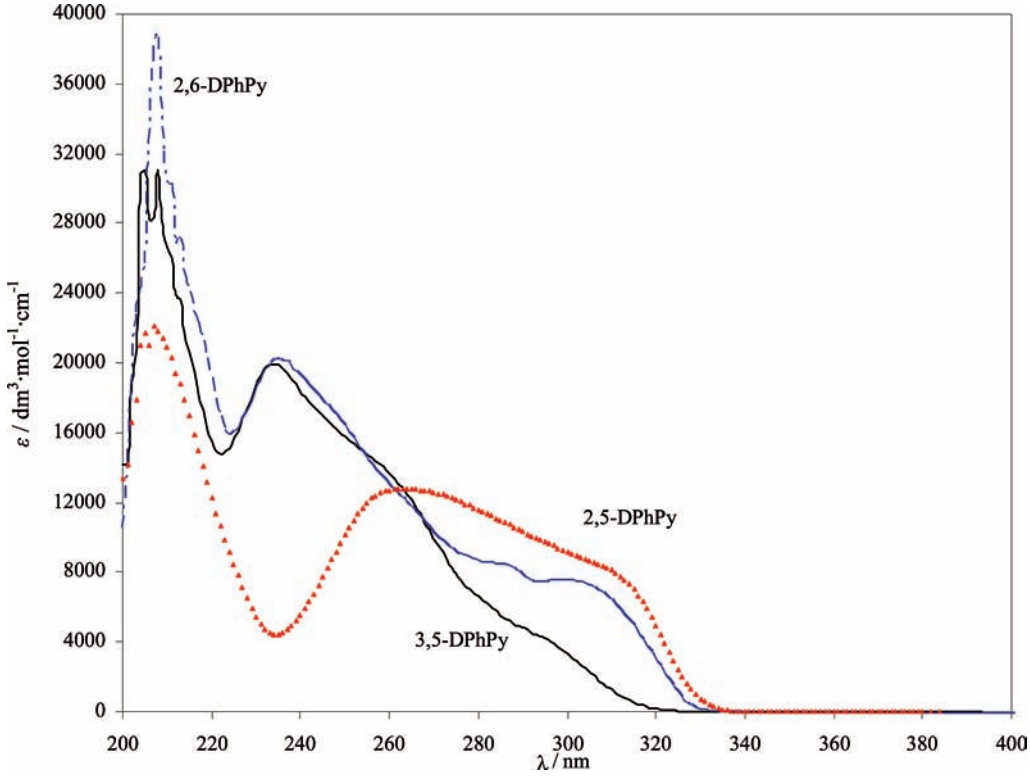

Figure 8. UV−vis spectra of the studied isomers in ethanol.

TABLE 5: Standard ($p^\circ = 0.1$ MPa) Molar Enthalpies of Sublimation, $\Delta^g_{cr}H_m^\circ$, at Reference Temperature $T = 298.15$ K, Determined by Calvet Microcalorimetry of 2,6-DPhPy, 2,5-DPhPy, and 3,5-DPhPy[a]

compound	no. of expts	T/K	$\Delta^{g,T}_{cr,\,298.15\,K}H_m^\circ$/kJ·mol^{-1}	$\Delta^T_{298.15\,K}H_m^\circ$(g)/kJ·mol^{-1}	$\Delta^g_{cr}H_m^\circ$(298.15 K)/kJ·mol^{-1}
2,6-DPhPy	6	432.4	155.3 ± 1.0	41.4 ± 1.0	114.0 ± 2.8
2,5-DPhPy	5	432.4	165.1 ± 1.0	41.4 ± 1.0	123.7 ± 2.8
3,5-DPhPy	5	432.5	170.6 ± 1.0	41.3 ± 1.0	129.3 ± 2.9

[a] The overall uncertainty includes the uncertainty of the calibration experiments, the uncertainty of the standard molar enthalpy of sublimation of anthracene, and the uncertainty associated with the molar enthalpic correction.

TABLE 6: Standard Molar Enthalpies, For the Condensed Phase, from the $T = 298.15$ K to the Temperature, T, Programmed in the Calvet Microcalorimeter, $\Delta^T_{298.15\,K}H_m^\circ$(cd), of 2,6-DPhPy, 2,5-DPhPy and 3,5-DPhPy

compound	T/K	$\langle T\rangle$/K	$\Delta^T_{298.15\,K}H_m^\circ$ (cd)/kJ·mol^{-1}
2,6-DPhPy	380.51	339.3	50.5 ± 0.8[a]
2,5-DPhPy	421.97	360.1	43.4 ± 0.3
3,5-DPhPy	384.49	341.3	27.5 ± 0.5

[a] The value $\Delta^T_{298.15\,K}H_m^\circ$(cd) of 2,6-DPhPy includes the values of $\Delta^{T_{fus}}_{298.15\,K}H_m^\circ$(cr), $\Delta^T_{T_{fus}}H_m^\circ$(l), and $\Delta^l_{cr}H_m^\circ(T_{fus})$.

TABLE 7: Experimental Data of Vapor Pressure for 2,6-DPhPy, 2,5-DPhPy, and 3,5-DPhPy

T/K	p/Pa	T/K	p/Pa
	2,6-DPhPy(l)		
360.71	0.456	382.50	2.484
362.69	0.535	384.48	2.879
364.68	0.624	386.45	3.315
366.65	0.738	388.44	3.824
368.64	0.859	390.42	4.391
370.62	1.006	392.39	5.043
372.59	1.172	394.38	5.776
374.57	1.362	396.35	6.582
376.57	1.597	398.34	7.523
378.55	1.846	400.31	8.586
380.53	2.153		
	2,5-DPhPy(cr)		
407.18	4.690	426.95	22.81
412.13	7.086	431.85	32.85
417.05	10.63	436.75	46.75
422.00	15.44		
	3,5-DPhPy(cr)		
369.64	0.281	387.46	1.758
372.61	0.387	390.43	2.361
375.59	0.533	393.41	3.145
378.56	0.712	396.37	4.152
381.53	0.972	399.34	5.474
384.50	1.314		

The value $\Delta^T_{298.15\,K}H_m^\circ$(cd) of 2,6-DPhPy corresponds to the heating of the compound in the crystalline phase, from $T = 298.15$ K to the fusion temperature ($T = 354.41$ K), due to the fusion and finally the heating of the liquefied compound, from the fusion temperature ($T = 354.41$ K) to the programmed temperature in the microcalorimeter, $T = 380.51$ K. The values $\Delta^T_{298.15\,K}H_m^\circ$(cd) of 2,5-DPhPy and 3,5-DPhPy correspond to the heating of the compound, in the crystalline phase, from $T = 298.15$ K to the programmed temperature in the microcalorimeter, $T = 421.97$ K for 2,5-DPhPy and $T = 384.49$ K in the case of 3,5-DPhPy.

The vapor pressures for the three isomers were measured at several temperatures, using the static apparatus based on an MKS capacitance diaphragm manometer. The integrated form of the Clausius−Clapeyron equation, eq 2, was used to derive the standard molar enthalpies of sublimation/vaporization at the mean temperature, $\langle T\rangle$, for 2,6-DPhPy(l), 2,5-DPhPy(cr), and 3,5-DPhPy(cr):

$$\ln(p/\text{Pa}) = a - b[(T/\text{K})^{-1}] \qquad (2)$$

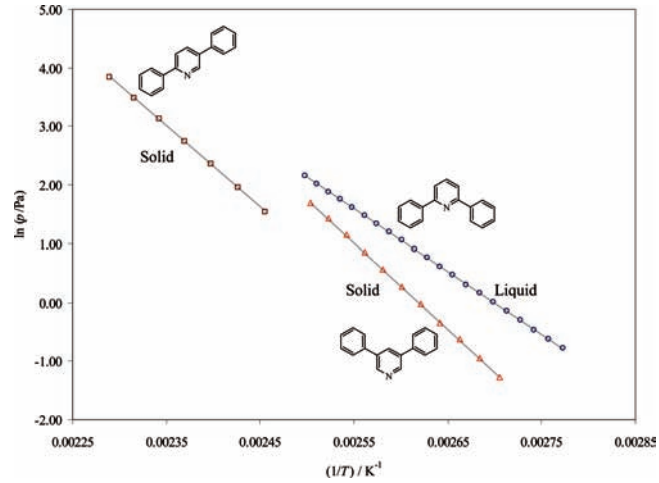

Figure 9. Plots of $\ln(p/\text{Pa})$ versus $(1/T)/\text{K}^{-1}$ for the studied isomers.

where a is a constant and $b = \Delta^g_{cd}H_m^\circ(\langle T\rangle)/R$. The experimental data of vapor pressures, for each studied compound, are presented in Table 7. The $\ln(p/\text{Pa}) = f[(T/\text{K})^{-1}]$ plots for the global results obtained for the studied isomers are presented in Figure 9. Table 8 lists the parameters of the Clausius−Clapeyron equation, the calculated standard deviations,and the standard molar enthalpies and entropies of sublimation/vaporization at the mean temperature, $\langle T\rangle$. The standard molar enthalpies of sublimation/vaporization at the mean temperature, $\Delta^g_{cd}H_m^\circ(\langle T\rangle)$, are calculated using the parameter b of the Clausius−Clapeyron equation, and the molar entropies of sublimation/vaporization at $p(\langle T\rangle)$ and at the mean temperature, $\Delta^g_{cd}S_m$ ($\langle T\rangle$, $p(\langle T\rangle)$), are calculated by eq 3:

$$\Delta^g_{cd}S_m(\langle T\rangle, p(\langle T\rangle)) = \Delta^g_{cd}H_m^\circ(\langle T\rangle)/\langle T\rangle \qquad (3)$$

The standard molar enthalpies of sublimation, at $T = 298.15$ K, are determined by eq 4:

$$\Delta^g_{cr}H_m^\circ(T = 298.15\ \text{K}) = \Delta^g_{cd}H_m^\circ(\langle T\rangle) + \left\lfloor\Delta^T_{298.15\,K}H_m^\circ(\text{cd}) - \Delta^T_{298.15\,K}H_m^\circ(\text{g})\right\rfloor \qquad (4)$$

where $\Delta^T_{298.15\,K}H_m^\circ$(cd) is the enthalpy change due to the heating of the sample, for the condensed phase, from $T = 298.15$ K to the temperature, T, determined experimentally by Calvet microcalorimetry (Table 6), and $\Delta^T_{298.15\,K}H_m^\circ$(g) is the enthalpy change due to the heating of the sample in the gaseous phase, from $T = 298.15$ K to the temperature, T, estimated computationally: $\Delta^T_{298.15\,K}H_m^\circ$(2,6-DPhPy, g) = (23.2 ± 1.0) kJ·mol^{-1}, $\Delta^T_{298.15K}H_m^\circ$(2,5-DPhPy, g) = (37.0 ± 1.0) kJ·mol^{-1}, and $\Delta^T_{298.15\,K}H_m^\circ$(3,5-DPhPy, g) = (24.4 ± 1.0) kJ·mol^{-1}.

TABLE 8: Experimental Results for the Studied Compounds, Where *a* and *b* Are from the Clausius−Clapeyron Equation: $\ln(p/\mathrm{Pa}) = a - b(\mathrm{K}/T)$[a]

a	b/K	r^2	$\langle T\rangle$/K	$p(\langle T\rangle)$/Pa	$\Delta_l^g H_m^\circ(\langle T\rangle)$/kJ·mol^{-1}	$\Delta_l^g S_m(\langle T\rangle;p(\langle T\rangle))$/J·K^{-1}·mol^{-1}
				2,6-DPhPy (l)		
28.98 ± 0.03	10 737 ± 11	0.9999	380.51	2.139	89.3 ± 0.1	234.6 ± 0.2
a	b/K	r^2	$\langle T\rangle$/K	$p(\langle T\rangle)$/Pa	$\Delta_{cr}^g H_m^\circ(\langle T\rangle)$/kJ·mol^{-1}	$\Delta_{cr}^g S_m(\langle T\rangle;p(\langle T\rangle))$/J·K^{-1}·mol^{-1}
				2,5-DPhPy (cr)		
35.51 ± 0.10	13 826 ± 43	0.9999	421.97	15.491	115.0 ± 0.4	272.4 ± 0.9
				3,5-DPhPy (cr)		
38.66 ± 0.06	14 759 ± 24	0.9999	384.49	1.313	122.7 ± 0.2	319.2 ± 0.5

[a] $b = \Delta_{cr}^g H_m^\circ(\langle T\rangle)/R$ or $b = \Delta_l^g H_m^\circ(\langle T\rangle)/R$; $R = 8.314\,472$ J·K^{-1}·mol^{-1}.

TABLE 9: Standard Molar Enthalpies, Entropies, and Gibbs Energies of Sublimation, at $T = 298.15$ K, for 2,6-DPhPy, 2,5-DPhPy, and 3,5-DPhPy

compound	$\Delta_{cr}^g H_m^\circ$/kJ·mol^{-1}	$\Delta_{cr}^g S_m^\circ$/J·K^{-1}·mol^{-1}	$\Delta_{cr}^g G_m^\circ$/kJ·mol^{-1}
2,6-DPhPy	116.6 ± 1.3	226.9 ± 5.4[a]	49.0 ± 1.0[a]
2,5-DPhPy	121.4 ± 1.1	216.6 ± 2.2	56.8 ± 1.3
3,5-DPhPy	125.8 ± 1.1	233.7 ± 2.1	56.1 ± 1.3

[a] Estimated values by extrapolation of the solid−vapor equilibrium line of 2,6-diphenylpyridine.

The standard molar entropies of sublimation, at $T = 298.15$ K, for 2,5-DPhPy and 3,5-DPhPy were calculated by the following equation:

$$\Delta_{cr}^g S_m^\circ(T = 298.15\ \mathrm{K}) = \Delta_{cr}^g S_m(\langle T\rangle, p(\langle T\rangle)) + \Delta_{cr}^g C_{p,m}^\circ \ln(298.15\ \mathrm{K}/\langle T\rangle) - R\ln\{p^\circ/p(\langle T\rangle)\} \quad (5)$$

with $\Delta_{cr}^g Cp,m^\circ = Cp,m^\circ(g) - Cp,m^\circ(cr)$ and $p^\circ = 0.1$ MPa. The $\Delta_{cr}^g Cp,m^\circ$ values for 2,5-DPhPy and 3,5-DPhPy were calculated using the experimental values of $C_{p,m}^\circ$(cr), Cp,m°(2,5-DPhPy, cr) = (347.8 ± 2.8) J·K^{-1}·mol^{-1} and Cp,m°(2,5-DPhPy, cr) = (314.0 ± 6.4) J·K^{-1}·mol^{-1}, and the heat capacity in gaseous phase derived from the ab initio calculations for the Cp,m°(g) values, Cp,m°(2,5-DPhPy, g) = (298.5 ± 5.0) J·K^{-1}·mol^{-1} and Cp,m°(2,5-DPhPy, g) = (282.5 ± 5.0) J·K^{-1}·mol^{-1}. Considering the values of Cp,m°(cr) and Cp,m°(g) presented above, the $\Delta_{cr}^g Cp,m^\circ$ values for 2,5-DPhPy and 3,5-DPhPy were derived: $\Delta_{cr}^g Cp,m^\circ$(2,5-DPhPy) = −(49.3 ± 5.7) J·K^{-1}·mol^{-1} and $\Delta_{cr}^g Cp,m^\circ$(3,5-DPhPy) = −(31.5 ± 8.1) J·K^{-1}·mol^{-1}.

The standard molar Gibbs energies of sublimation, at $T = 298.15$ K, of 2,5-DPhPy and 3,5-DPhPy, were calculated using eq 6, where the standard molar enthalpies and standard molar entropies of sublimation are referred to the reference temperature, $T = 298.15$ K, and standard pressure, $p^\circ = 0.1$ MPa. Table 9 lists the standard molar enthalpies, entropies, and Gibbs energies of sublimation for all studied isomers. The values of the standard molar entropy and the Gibbs energy of sublimation for 2,6-DPhPy were estimated by extrapolation of the estimated solid−vapor equilibrium line of the isomer.

$$\Delta_{cr}^g G_m^\circ = \Delta_{cr}^g H_m^\circ - 298.15\Delta_{cr}^g S_m^\circ \quad (6)$$

Comparing the values of standard molar enthalpies of sublimation obtained by Calvet microcalorimetry and the static apparatus, for the three compounds studied, it can be verified that the obtained data concerning the sublimation are in agreement, given the uncertainty range. A gradual decrease of the standard molar enthalpies of sublimation is found when the phenyl rings are positioned adjacent to the nitrogen atom of the pyridine ring: 2,6-DPhPy < 2,5-DPhPy < 3,5-DPhPy. Analyzing the values of the standard molar entropies of sublimation, a gradual increase can be verified in accordance with the following sequence: 2,5-DPhPy < 2,6-DPhPy < 3,5-DPhPy. The absolute standard molar entropies in the gaseous phase, S_m°(g), should be identical for the three isomers; therefore, the following order of absolute standard molar entropies in the crystalline phase, S_m°(cr) are derived: 2,5-DPhPy > 2.6-DPhPy > 3,5-DPhPy. The observed orders for the enthalpic and entropic contributions associated to the respective sublimation processes are in agreement with the same order for the thermodynamic properties observed in the fusion equilibria and supported by the crystal packing. The 2,6-DPhPy isomer, in which two C−H···N intramolecular interactions and a weak C−H···π intermolecular interaction were found, presents a more flat molecular geometry,[40] a lower density in the crystalline phase, and a lower standard molar enthalpy of sublimation. The 3,5-DPhPy crystal structure shows a $\pi\cdots\pi$ intermolecular interaction between a top adjacent folded pyridine and two weak C−H···π intermolecular interactions, and it is the isomer with the highest standard molar enthalpy of fusion and sublimation. The entropic contribution associated with the central ring disorder observed by X-ray diffraction in 2,5-DPhPy is in agreement with the highest absolute standard molar entropy in the crystalline phase. The low volatility and the highest temperature of fusion are ruled by the highest absolute standard molar entropy in the crystalline phase of the 2,5-DPhPy isomer, as can be observed in the position of the triple point in Figure 10.

Using the thermodynamic parameters of sublimation/vaporization and the values of standard molar enthalpies of fusion, the solid−vapor equilibrium of 2,6-DPhPy and the liquid−vapor equilibria of 2,5-DPhPy and 3,5-DPhPy were derived. The triple points, solid−vapor equilibria lines, and liquid−vapor equilibria lines are presented in the phase diagram (Figure 10) where the standard molar Gibbs energy is plotted as a function of the absolute temperature ($\Delta_{cd}^g G_m^\circ/\mathrm{kJ\cdot mol^{-1}} = f(T/\mathrm{K})$).

The isomer with the molecular linear shape, 2,5-DPhPy (phenyl groups in para position), presents a liquid−vapor equilibrium line close to the lines of equilibrium of the other isomers, showing nevertheless a lower liquid volatility, being in agreement with the expected highest absolute entropy. The liquid−vapor equilibrium lines for 2,6-DPhPy and 3,5-DPhPy (phenyl groups in meta position, "V"-shape structure) are nearly coincident; therefore they have a very similar volatility.

Molecular Energetics. Table 10 reports on typical experimental combustion results for each studied isomer, where $\Delta m(H_2O)$ is the deviation from the average mass of water (2900.0 g) added to the calorimeter, which is the mass assigned

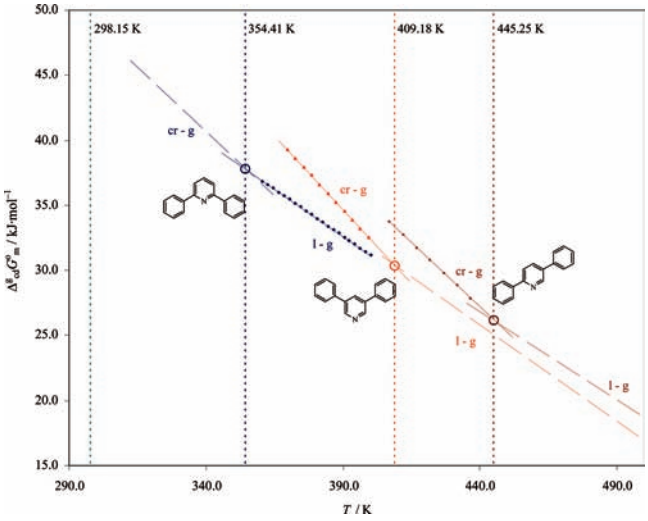

Figure 10. Plots of standard molar phase change Gibbs energies versus temperature ($\Delta^{g}_{cd}G_m^\circ$/kJ·mol^{-1} = $f(T$/K)).

TABLE 10: Typical Experimental Results at T = 298.15 K (p° = 0.1 MPa)[a]

	2,6-DPhPy	2,5-DPhPy	3,5-DPhPy
m(cpd)/g	0.339 80	0.442 46	0.482 57
m'(fuse)/g	0.003 16	0.002 96	0.002 94
m''(BA)/g	0.198 77	–	–
T_i/K	298.149 88	298.149 97	298.150 06
T_f/K	299.396 69	299.309 11	299.407 84
ΔT_{ad}/K	1.169 06	1.079 07	1.181 12
ε_i(cont)/J·K^{-1}	13.59	13.47	13.52
ε_f(cont)/J·K^{-1}	14.12	13.90	13.97
Δm(H_2O)/g	−3.0	−3.7	−9.1
$-\Delta U$(IBP)[b]/J	18 176.44	16 773.89	18 333.72
ΔU(fuse)/J	51.24	48.07	47.75
ΔU(BA)/J	5254.36	–	–
ΔU(HNO_3)/J	16.85	19.92	23.31
ΔU(ign)/J	0.88	1.18	0.83
$-\Delta U$(carb)/J	0.00	0.00	0.00
ΔU_Σ/J	11.64	9.99	10.97
$-\Delta_c u^\circ$(cpd)/J·g^{-1}	37 791.26	37 731.61	37 820.13

[a] m(cpd) is the mass of compound burned in each experiment, m'(fuse) is the mass of the fuse (cotton) used in each experiment, m''(BA) is the mass of benzoic acid used in each experiment, T_i is the initial temperature rise, T_f is the final temperature rise, ΔT_{ad} is the corrected temperature rise, ε_i(cont) is the energy equivalent of the contents in the initial state, ε_f(cont) is the energy equivalent of the contents in the final state, Δm(H_2O) is the deviation of the mass of water added to the calorimeter from 2900.0 g, ΔU(IBP) is the energy change for the isothermal combustion reaction under actual bomb conditions, ΔU(HNO_3) is the energy correction for nitric acid formation, ΔU(ign) is the electric energy for ignition, ΔU^a is the standard-state correction, $\Delta_c u^\circ$(fuse) is the massic energy of combustion of the fuse (cotton), and $\Delta_c u^\circ$ is the standard massic energy of combustion. [b] ΔU(IBP) includes ΔU(ign).

to ε(calor); the remaining terms are as previously described.[23] The full sets of experimental data are available in Tables S3−S5 in the Supporting Information.

The internal energy associated with the isothermal bomb process, ΔU(IBP), was calculated according to the following equation:

$$\Delta U(\text{IBP}) = -[\varepsilon(\text{calor}) + c_p(H_2O, l)\,\Delta m(H_2O)]\Delta T_{ad} + (T_i - 298.15)\varepsilon_i + (298.15 - T_i - \Delta T_{ad})\varepsilon_f + \Delta U(\text{ign}) \quad (7)$$

TABLE 11: Individual Values of the Standard (p° = 0.1 MPa) Massic Energy of Combustion, $\Delta_c u^\circ$, of the Three Diphenylpyridine Isomers at T = 298.15 K

$\Delta_c u^\circ$/(J·g^{-1})		
2,6-DPhPy	2,5-DPhPy	3,5-DPhPy
−37 791.26	−37 731.61	−37 820.13
−37 798.89	−37 739.10	−37 790.74
−37 774.23	−37 733.56	−37 810.15
−37 762.47	−37 749.80	−37 820.12
−37 795.68	−37 742.20	−37 817.02
−37 779.70		−37 803.01
−37 803.88		−37 788.44
−37 789.91		
−37 774.64		
$\langle\Delta_c u^\circ\rangle$[a]/(J·g^{-1})		
2,6-DPhPy	2,5-DPhPy	3,5-DPhPy
−37 785.6 ± 4.5	−37 739.3 ± 3.2	−37 807.1 ± 5.1

[a] Mean value and given error as the standard deviation of the mean.

TABLE 12: Derived Standard Molar Energies of Combustion, $\Delta_c U_m^\circ$(cr), Standard Molar Enthalpies of Combustion, $\Delta_c H_m^\circ$(cr), and Standard Molar Enthalpies of Formation in Crystal Phase, $\Delta_f H_m^\circ$(cr), at Reference Temperature, T = 298.15 K

compound	$-\Delta_c U_m^\circ$(cr)/ kJ·mol^{-1}	$-\Delta_c H_m^\circ$(cr)/ kJ·mol^{-1}	$\Delta_f H_m^\circ$ (cr)/ kJ·mol^{-1}
2,6-DPhPy	8739.6 ± 4.1	8746.4 ± 4.1	198.8 ± 4.6
2,5-DPhPy	8728.8 ± 3.0	8735.7 ± 3.0	188.1 ± 3.8
3,5-DPhPy	8744.5 ± 3.9	8751.3 ± 3.9	203.8 ± 4.5

where ΔT_{ad} is the calorimeter temperature change corrected for the heat exchange and the work of stirring, calculated with the software LABTERMO V3.0 using the Regnault−Pfaundler method, applying a second-order fitting for the initial and final periods, as reported by Santos et al.[20]

For each isomer, the products of the combustion experiments consist of a gaseous phase and an aqueous mixture of nitric acid, for which the thermodynamic properties are known. The values of $\Delta_c u^\circ$ refer to the reaction represented by

$$C_{17}H_{13}N(cr) + \frac{81}{4}O_2(g) \rightarrow 17CO_2(g) + \frac{13}{2}H_2O(l) + \frac{1}{2}N_2(g) \quad (8)$$

The individual values of $\Delta_c u^\circ$, the mean, and the standard deviation of the mean are listed in Table 11. The derived standard molar energies of combustion, $\Delta_c U_m^\circ$(cr), the standard molar enthalpies of combustion, $\Delta_c H_m^\circ$(cr), and the standard molar enthalpies of formation in the crystal phase, $\Delta_f H_m^\circ$(cr), at the reference temperature, T = 298.15 K, are listed in Table 12. In Table 13, the values of standard molar enthalpies of sublimation, $\Delta^g_{cr}H_m^\circ$, obtained with the two techniques, and the derived standard molar enthalpies of formation in the gaseous phase, $\Delta_f H_m^\circ$(g), at T = 298.15 K, are presented. In accordance with the thermochemical practice, the uncertainties assigned to the standard molar enthalpies of combustion and formation are twice the overall standard deviation of the mean and include the uncertainties in the calibration and in the auxiliary quantities used. To derive $\Delta_f H_m^\circ$(cr) from $\Delta_c H_m^\circ$(cr), the standard molar enthalpies of formation of H_2O(l) and CO_2(g) at T = 298.15 K, −(285.830 ± 0.13) kJ·mol^{-1} and −(393.51 ± 0.040) kJ·mol^{-1},[41] respectively, were used.

TABLE 13: Standard Molar Enthalpies of Sublimation, $\Delta_{cr}^{g}H_m°$, and Derived Standard Molar Enthalpies of Formation in the Gaseous Phase at 298.15 K

		Calvet microcalorimeter		static apparatus	
compound	$\Delta_fH_m°$(cr)/kJ·mol^{-1}	$\Delta_{cr}^{g}H_m°$/kJ·mol^{-1}	$\Delta_fH_m°$(g)/kJ·mol^{-1}	$\Delta_{cr}^{g}H_m°$/kJ·mol^{-1}	$\Delta_fH_m°$(g)/kJ·mol^{-1}
2,6-DPhPy	198.8 ± 4.6	114.0 ± 2.8	312.8 ± 5.4	116.6 ± 1.3	315.4 ± 4.8
2,5-DPhPy	188.1 ± 3.8	123.7 ± 2.8	311.8 ± 5.0	121.4 ± 1.1	309.5 ± 4.2
3,5-DPhPy	203.8 ± 4.5	129.3 ± 2.9	333.1 ± 5.4	125.8 ± 1.1	329.6 ± 4.6

TABLE 14: Experimental and Theoretical Inter-ring Dihedral Angles (deg) for the Three Isomers

compound		X-ray	B3LYP/6-311++G(d,p)	MP2/cc-pVDZ
2,6-DPhPy	φ(N1−C6−C61−C66)	25.0[40]	24.5	27.9
	φ(N1−C2−C21−C26)	28.5[40]	24.5	27.9
2,5-DPhPy	φ(N1A−C2−C21−C26)	−	20.9	24.9
	φ(C1B−C2−C21−C22)	−	39.6	42.0
3,5-DPhPy	φ(C2−C3−C31−C32)	32.67	41.4	42.9
	φ(C2a−C3a−C31a−C32a)	32.67	41.4	42.9

For the energetic analysis in the gaseous phase, the following values of $\Delta_fH_m°$(g) were considered: (312.8 ± 5.4) kJ·mol^{-1} for 2,6-DPhPy, (309.5 ± 4.2) kJ·mol^{-1} for 2,5-DPhPy, and (329.6 ± 4.6) kJ·mol^{-1} for 3,5-DPhPy.

The values of $\Delta_fH_m°$(g) indicate 3,5-DPhPy as being the most unstable isomer in the gaseous phase. The higher enthalpic stability evidenced on the 2,6-DPhPy isomer is associated with the existence of two intramolecular C−H···N interactions between the phenyl group and the nitrogen atom of the pyridine ring. The enthalpic contribution of this type of interaction has also been observed in a previous study on the phenylpyridine isomers.[4]

The relative enthalpic stability of the 2,5-DPhPy locates this isomer with a gaseous phase stability identical with the one observed in the 2,6-DPhPy isomer. In the 2,5-DPhPy isomer, an intramolecular C−H···N interaction between the adjacent phenyl group and the nitrogen atom of the pyridine ring, and a higher conjugation between the aromatic rings in para position was found. This higher conjugation observed in the 2,5-DPhPy isomer is energetically supported, as well as by comparative analysis of the UV−vis spectra.

The standard molar enthalpies of formation in gaseous phase, at T = 298.15 K, for the three isomers, were also computationally estimated, using density functional theory (DFT) with the hybrid exchange correlation functional (B3LYP), second-order Møller−Plesset perturbation theory (MP2), and spin-component-scaled MP2 (SCS-MP2).

Computational Results. The molecular structures in the gaseous phase, for the studied isomers, were obtained through full geometry optimizations, carried out using B3LYP/6-311++G(d,p) and MP2/cc-pVDZ levels of theory. For all isomers, the different combinations of cis and trans conformations of the ring geometries were explored. A very small (on the order of 0.5 mhartree) minimum electronic energy differentiation between the different conformations was found. In all cases, the cis conformation was the more stable conformation. Table 14 lists the dihedral angles obtained by ab initio calculations and by X-ray diffraction.

For 2,6-DPhPy, a good agreement was observed between the experimental dihedral angles (obtained by X-ray diffractometry in the crystal) with those obtained computationally at different levels of theory, for the gaseous phase. The theoretical geometry optimization at this level of theory describes quite reasonably the two intramolecular C−H···N interactions in 2,6-DPhPy. The inter-ring dihedral angles obtained by ab initio calculations in the gaseous phase are significantly higher than the ones obtained experimentally in the crystalline phase of 3,5-DPhPy. This difference is related to the low ring rotational barrier of the phenyl rings in 3,5-DPhPy in the gaseous phase.

The X-ray crystal structure of 2,5-DPhPy presents two twisted conformations that are distinguished by the inter-ring (phenyl and pyridine) dihedral angle, in which one of the conformations is more planar than the other. In this case, it is meaningless to compare the dihedral angles obtained experimentally and theoretically for the 2,5-DPhPy isomer. The inter-ring dihedral angle relative to the phenyl group adjacent to the nitrogen atom obtained by ab initio calculations for 2,5-DPhPy is lower than the one obtained for 2,6-DPhPy. The higher dihedral angle observed in the 2,6-DPhPy isomer is associated with the existence of two simultaneous symmetrical C−H···N intramolecular interactions in cis conformation of the phenyl rings. For the 2,5-DPhPy isomer, the smaller dihedral angle observed between the adjacent phenyl ring to the nitrogen atom in the pyridine could be related to the unconstrained C−H···N interaction.

The zero-point energy correction (ZPE), the total electronic energy plus zero-point energy correction (E_0 + ZPE), and the enthalpic correction for thermal vibration at 298.15 K ($H_{298.15\,K}$), obtained from the geometry optimizations of the selected compounds and for different levels of theory, are available in Table S6 in the Supporting Information. The computationally obtained standard molar enthalpies of formation in the gaseous phase, $\Delta_fH_m°$(g), for the three isomers, were calculated based on the homodesmic reaction scheme presented in Figure 11. Table 15 lists the calculated values at different levels of theory and the experimental values of $\Delta_fH_m°$(g) at the reference temperature, T = 298.15 K. For the calculation of $\Delta_fH_m°$(g), the following literature values (in kJ·mol^{-1}) of $\Delta_fH_m°$(g) at T = 298.15 K were used: benzene, (82.6 ± 0.7) kJ·mol^{-1};[42] biphenyl, (181.4 ± 2.0) kJ·mol^{-1};[42] pyridine, (140.4 ± 0.7) kJ·mol^{-1}.[42]

The theoretical enthalpies of formation, $\Delta_fH_m°$(g), are systematically higher than the experimental results, showing that the levels of theory used in this work underestimate the relative energetic stability associated with aromatic conjugation between the rings. Therefore, any attempt to use the computational results in order to evaluate the energetic differentiation arising from the phenyl conjugation is meaningful.

The NICS-scan plots for the three isomers in the cis and trans conformation and for pyridine are available as Supporting Information. Table 16 lists the NICS values for the pyridine ring for each isomer.

Analyzing the NICS values, it can be shown that all the isomers present a lower aromaticity than the pyridine. The decrease of the aromaticity follows the order 3,5-DPhPy > 2,5-

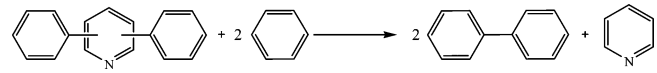

Figure 11. Homodesmic reaction in the gas phase, involving the isomers at standard conditions at reference temperature, T = 298.15 K.

TABLE 15: Experimental and Computed Values of $\Delta_f H_m°(g)$ at $T = 298.15$ K for the Three Studied Isomers

	$\Delta_f H_m°(g)$/kJ·mol^{-1}										
		B3LYP		MP2		SCS-MP2		MP2		SCS-MP2	
compound	experimental	6-311++G(d,p)	Δ^a	cc-pVDZ	Δ^a	cc-pVDZ	Δ^a	6-311++G(d,p)	Δ^a	6-311++G(d,p)	Δ^a
2,6-DPhPy	312.8 ± 5.4	323.6	−10.8	326.0	−13.2	324.1	−11.3	333.1	−20.3	329.3	−16.5
2,5-DPhPy	309.5 ± 4.2	328.8	−19.3	330.7	−21.2	329.7	−20.2	337.8	−28.3	334.8	−25.3
3,5-DPhPy	329.6 ± 4.6	337.2	−7.6	336.7	−7.1	337.3	−7.7	340.2	−10.6	339.7	−10.1

[a] $\Delta = \Delta_f H_m°$(g, experimental) − $\Delta_f H_m°$(g, theoretical).

TABLE 16: NICS Values for Pyridine and for the Three Studied Isomers, at the B3LYP/6-311++G(d,p) Level of Theory

compound	NICS (−1)	NICS (0)	NICS (1)
Py	−10.2	−6.8	−10.2
2,6-DPhPy (*cis*)	−8.4	−4.6	−7.9
2,5-DPhPy (*cis*)	−8.7	−5.2	−8.4
3,5-DPhPy (*cis*)	−9.1	−6.1	−8.9
2,6-DPhPy (*trans*)	−8.0	−4.5	−8.0
2,5-DPhPy (*trans*)	−8.4	−5.2	−8.6
3,5-DPhPy (*trans*)	−9.1	−6.3	−9.1

DPhPy > 2,6-DPhPy, in agreement with the order of the expected magnitude of the σ and π conjugation between the phenyl rings and the nitrogen atom (more electronegative than the carbon atom) of the pyridine ring and therefore the increase of the asymmetrical shape of the charge density in the pyridine. The 3,5-DPhPy isomer, in which the phenyl rings are in meta position (relative to the nitrogen atom of the central ring), is the one with the higher aromaticity in the pyridine ring. The 2,6-DPhPy isomer, in which both phenyl groups are in ortho position relative to the nitrogen atom of the pyridine ring, presents the lower aromaticity in the pyridine ring. The 2,5-DPhPy isomer is in the intermediate situation, with the phenyl groups in both ortho and meta positions relative to the nitrogen atom of the central ring. For the studied isomers, the cis conformation geometry presents an asymmetry in the NICS values (Table 16) between the parts above and below the pyridine ring. This asymmetry in the profiles of the NICS values reflects the asymmetric (above and below) shape of the charge density in the pyridine.

Final Remarks

The characterization of the title isomers by X-ray diffractometry, spectroscopic and experimental thermodynamics techniques, as well as ab initio calculations allows the discussion of the relationships between their structures and energetics. In the solid state, the supramolecular structure is stabilized by C−H···π intermolecular interactions for all isomers. Besides this, some special features are observed in the crystal packing of the individual compounds that can be systemized in order to explain some of the observed differences in their thermodynamic properties: (i) In 2,6-DPhPy, two intramolecular C−H···N interactions are observed. (ii) 2,5-DPhPy, isomorphic with the corresponding polyphenyl hydrocarbon, shows a herringbone pattern packing typical for aromatic hydrocarbon compounds. The molecule is disordered in the cell and presents two different conformations. (iii) The 3,5-DPhPy isomer shows an extra C−H···π interaction and a π···π interaction between the pyridine rings. The structural differences in the supramolecular assemblies are primarily reflected in the phase transition thermodynamics, namely the temperatures of fusion, standard molar enthalpies and entropies of fusion, as well as vapor pressures, standard molar enthalpies, entropies, and Gibbs energies of sublimation. The extra intermolecular C−H···π interaction and the intermolecular π···π interaction observed for 3,5-DPhPy appear to raise the standard molar enthalpy of fusion as well as the enthalpy of sublimation of this isomer, while the disorder associated with 2,5-DPhPy leads to a high absolute standard molar entropy in the crystalline phase, and lowers its volatility and the standard molar enthalpy and entropy of sublimation. The relative positions of the phenyl rings in the pyridine ring were used to rationalize the molecular structure, energetics, and phase diagram, based on the specific molecular inter-ring aromatic conjugation, C−H···N intramolecular interactions, and C−H···π and π···π intermolecular interactions.

The location of the two phenyl rings in adjacent positions relative to the nitrogen atom of the pyridine as well as the intramolecular C−H···N interactions in the 2,6-DPhPy isomer gives rise to the high enthalpic stability in the gaseous phase, taking into account the experimentally obtained lower standard molar enthalpy of formation in the gaseous phase, when compared with 3,5-DPhPy. The 2,5-DPhPy isomer presents an enthalpic stability in the gaseous state similar to that of the 2,6-DPhPy isomer, and it seems to be the compound with the higher aromatic conjugation, as suggested by its energetic stability, UV−vis data, and structural isomorphism with *p*-terphenyl. In order to understand the effect of the position of the phenyl groups relative to the heteroatom on the aromaticity of the central ring, calculations of NICS values were also performed for the three isomers. The following order of aromaticity was found for the pyridine ring: 3,5-DPhPy > 2,5-DPhPy >2,6-DPhPy.

The obtained experimental results for the energetics in the gaseous phase of the three compounds were compared with the values obtained by ab initio calculations at different levels of theory (DFT and MP2), showing that, at these levels of theory, the computational methods underestimate the energetic stability in the gaseous phase for these aromatic compounds.

CCDC 722316 and CCDC 690365 contain the supplementary crystallographic data for this paper. These data can be obtained free of charge from The Cambridge Crystallographic Data Centre via www.ccdc.cam.ac.uk/data_request/cif.

Acknowledgment. Thanks are due to FCT, the Programa Operacional Ciência e Inovação 2010 (POCI2010), and FEDER for financial support to Project No. POCI/QUI/61873/2004, and CIQUP for financial support.

Supporting Information Available: Additional crystallographic data referring to the 2,5-and 3,5-diphenylpyridine isomers (Tables S1.1−S2.5). Thermochemical experimental data for the three studied isomers (Tables S3−S5). Zero-point energy correction (ZPE), total electronic energy plus zero-point energy correction, and enthalpic energy plus thermal correction at 298.15 K for the studied compounds (Table S6). NICS values for the scan from −2 to +2 Å from the aromatic plane (Table S7). Plot of the NICS values for the scan from −2 to +2 Å from the center of the benzene ring for each compound and the

optimized geometries (*xyz* format) and energies, obtained at the B3LYP/6-311++G(d,p) level, and *a* (Tables S7−S11.3 and Figures S1−S7). This material is available free of charge via the Internet at http://pubs.acs.org.

References and Notes

(1) Perez-Medina, L. A.; Merriella, R. P.; McElvain, S. M. *J. Am. Chem. Soc.* **1947**, *69*, 2574–2579.

(2) Jacquemard, U.; Routier, S.; Dias, N.; Lansiaux, A.; Goossens, J.-F.; Bailly, C.; Merour, J. Y. *Eur. J. Med. Chem.* **2005**, *40*, 1087–1095.

(3) Zuo, J.-L.; Yang, J.-X.; Wang, F.-Z.; Xiang-Nan; Dang, X.-N.; Sun, J.-L.; Zou, D.-C.; Tian, Y.-P.; Lin, N.; Tao, X.-T.; Jiang, M.-H. *J. Photochem. Photobiol. Chem.* **2008**, *199*, 322–329.

(4) Ribeiro da Silva, M. A. V.; Matos, M. A. R.; Rio, C. A.; Morais, V. M. F.; Wang, J.; Nichols, G.; Chickos, J. S. *J. Phys. Chem. A* **2000**, *104*, 1774–1778.

(5) (a) Miyaura, N.; Suzuki, A. *Chem. Rev.* **1995**, *95*, 2457–2483. (b) Suzuki, A. *J. Organomet. Chem.* **1999**, *576*, 147. (c) Liu, L.; Zhang, Y.; Xin, B. *J. Org. Chem.* **2006**, *71*, 3994–3997.

(6) Wieser, M. E. *Pure Appl. Chem.* **2006**, *78*, 2051–2066.

(7) Bruker. *Smart APEX* (version 5.62), *SAINT* (version 6.02), *SHELX-TL* (version 6.10), and *SADABS* (version 2.03); Bruker AXS Inc.: Madison, WI, 2004.

(8) Sheldrick, G. M. *SADABS—Bruker Nonius area detector scaling and absorption correction*, version 2.10; 2003.

(9) Sheldrick, G. M. *SHELXS97* and *SHELXL97*; University of Göttingen: Göttingen, Germany, 1997.

(10) Johnson, C. K.; Burnett, M. N. *ORTEPIII for Windows*; University of Glasgow: Glasgow, U.K., 1998.

(11) Spek, A. L. *J. Appl. Crystallogr.* **2003**, *36*, 7–13.

(12) Adedeji, F. A.; Lalage, D.; Brown, S.; Connor, J. A.; Leung, M. L.; Paz-Andrade, I. M.; Skinner, H. A. *J. Organomet. Chem.* **1975**, *97*, 221–228.

(13) Santos, L. M. N. B. F.; Schröder, B.; Fernandes, O. O. P.; Ribeiro da Silva, M. A. V. *Thermochim. Acta* **2004**, *415*, 15–20.

(14) Merrick, J. P.; Moran, D.; Radom, L. *J. Phys. Chem. A* **2007**, *111*, 11683–11700.

(15) Ribeiro da Silva, M. A. V.; Monte, M. J. S.; Santos, L. M. N. B. F. *J. Chem. Thermodyn.* **2006**, *38*, 778–787.

(16) Bernardes, C. E. S.; Santos, L. M. N. B. F.; Minas da Piedade, M. E. *Meas. Sci. Technol.* **2006**, *17*, 1405–1408.

(17) Monte, M. J. S.; Santos, L. M. N. B. F.; Fulem, M.; Fonseca, J. M. S.; Sousa, C. A. D. *J. Chem. Eng. Data* **2006**, *51*, 757–766.

(18) Gundry, H. A.; Harrop, D.; Head, A. J.; Lewis, G. B. *J. Chem. Thermodyn.* **1969**, *1*, 321–332.

(19) Bickerton, J.; Pilcher, G.; Al-Takhin, G. *J. Chem. Thermodyn.* **1984**, *16*, 373–378.

(20) Ribeiro da Silva, M. D. M. C.; Santos, L. M. N. B. F.; Silva, A. L. R.; Fernandes, O.; Acree, W. E., Jr. *J. Chem. Thermodyn* **2003**, *35*, 1093–1100.

(21) Santos, L. M. N. B. F.; Silva, M. T.; Schröder, B.; Gomes, L. *J. Therm. Anal. Calorim.* **2007**, *89*, 175–180.

(22) Coops, J.; Jessup, R. S.; van Nes, K. G. In *Experimental Thermochemistry*; Rossini, F. D., Ed.; Interscience: New York, 1956; Vol. 1, Chapter 3.

(23) Good, W. D.; Scott, D. W.; Waddington, G. *J. Phys. Chem.* **1956**, *60*, 1080–1089.

(24) Wagman, D. D.; Evans, W. H.; Parker, V. B.; Schumm, R. H.; Halow, I.; Bailey, S. M.; Churney, K. L.; Nuttall, R. L. *J. Phys. Chem. Ref. Data* **1982**, *11*, 2.

(25) Washburn, E. N. *J. Res. Natl. Bur. Stand. (U.S.)* **1933**, *10*, 525–558.

(26) Hubbard, W. N.; Scott, D. W.; Waddington, G. In *Experimental Thermochemistry*; Rossini, F. D., Ed.; Interscience: New York, 1956; Vol. 1, Chapter 5.

(27) Good, W. D.; Scott, D. W. In *Experimental Thermochemistry*; Skinner, H. A., Ed.; Interscience: New York, 1962; Vol. 2, Chapter 2.

(28) (a) Becke, A. D. *J. Chem. Phys.* **1993**, *98*, 5648–5652. (b) Becke, A. D. *Phys. Rev. A* **1988**, *38*, 3098–3100.

(29) (a) Møller, C.; Plesset, M. S. *Phys. Rev.* **1934**, *46*, 618–622. (b) Grimme, S. *J. Chem. Phys.* **2003**, *118*, 9095–9102.

(30) Schleyer, P. v. R.; Maerker, C.; Dransfeld, A.; Jiao, H.; Hommes, N. J. R. v. E. *J. Am. Chem. Soc.* **1996**, *118*, 6317–6318.

(31) Chen, Z.; Wannere, C. S.; Corminboeuf, C.; Puchta, R.; Schleyer, P. v. R. *Chem. Rev.* **2005**, *105*, 3842–3888.

(32) Lima, C. F. R. A. C.; Gomes, L. R.; Santos, L. M. N. B. F. *J. Phys. Chem. A* **2007**, *111*, 10598–10603.

(33) Stanger, A. *J. Org. Chem.* **2006**, *71*, 883–893.

(34) Frisch, M. J.; Trucks, G. W.; Schlegel, H. B.; Scuseria, G. E.; Robb, M. A.; Cheeseman, J. R.; Montgomery, J. A., Jr.; Vreven, T.; Kudin, K. N.; Burant, J. C.; Millam, J. M.; Iyengar, S. S.; Tomasi, J.; Barone, V.; Mennucci, B.; Cossi, M.; Scalmani, G.; Rega, N.; Petersson, G. A.; Nakatsuji, H.; Hada, M.; Ehara, M.; Toyota, K.; Fukuda, R.; Hasegawa, J.; Ishida, M.; Nakajima, T.; Honda, Y.; Kitao, O.; Nakai, H.; Klene, M.; Li, X.; Knox, J. E.; Hratchian, H. P.; Cross, J. B.; Bakken, V.; Adamo, C.; Jaramillo, J.; Gomperts, R.; Stratmann, R. E.; Yazyev, O.; Austin, A. J.; Cammi, R.; Pomelli, C.; Ochterski, J. W.; Ayala, P. Y.; Morokuma, K.; Voth, G. A.; Salvador, P.; Dannenberg, J. J.; Zakrzewski, V. G.; Dapprich, S.; Daniels, A. D.; Strain, M. C.; Farkas, O.; Malick, D. K.; Rabuck, A. D.; Raghavachari, K.; Foresman, J. B.; Ortiz, J. V.; Cui, Q.; Baboul, A. G.; Clifford, S.; Cioslowski, J.; Stefanov, B. B.; Liu, G.; Liashenko, A.; Piskorz, P.; Komaromi, I.; Martin, R. L.; Fox, D. J.; Keith, T.; Al-Laham, M. A.; Peng, C. Y.; Nanayakkara, A.; Challacombe, M.; Gill, P. M. W.; Johnson, B.; Chen, W.; Wong, M. W.; Gonzalez, C.; Pople, J. A. *Gaussian 03*, revision C.02; Gaussian, Inc.: Pittsburgh, PA, 2004.

(35) Baudour, J. L.; Toupet, L.; Délugeard, Y.; Guémid, S. *Acta Crystallogr.* **1986**, *C42*, 1211–1217.

(36) Baudour, J. L. *Acta Crystallogr.* **1991**, *B47*, 935–949.

(37) Desiraju, G. R.; Gavezzotti, A. *J. Chem. Soc., Chem. Commun.* **1989**, 621–623.

(38) Crispini, A.; Neve, F. *Acta Crystallogr.* **2002**, *C58*, o34–o35.

(39) Silva, A. M. S.; Almeida, L. M. P. M.; Cavaleiro, J. A. S.; Foces-Foces, C.; Liamas-Saiz, A. L.; Fontenas, C.; Jagerovic, N.; Elguero, J. *Tetrahedron* **1997**, *53*, 11645–11658.

(40) Rocha, M. A.; Low, J. N.; Gomes, L. R.; Quesada, A.; Santos, L. M. N. B. F. *Acta Crystallogr.* **2007**, *E63*, o4833.

(41) Cox, J. D., Wagman, D. D., Medvedev, V. A. *CODATA Key Values for Thermodynamics*; Hemisphere Publishing Corp.: New York, 1989.

(42) Pedley, J. B. *Thermochemical Data and Structures of Organic Compounds*; Thermodynamics Research Center: College Station, TX, 1994.

JP903792D